This is the peer reviewd version of the followng article:

Imaging haemodynamic changes related to seizures: Comparison of EEG-based general linear model, independent component analysis of fMRI and intracranial EEG / Thornton, R.C., Rodionov, R., Laufs, H., Vulliemoz, S., Vaudano, A.E., Carmichael, D., Cannadathu, S., Guye, M., Mcevoy, A., Lhatoo, S., Bartolomei, F., Chauvel, P., Diehl, B., De Martino, F., Elwes, R.D.C., Walker, M.C., Duncan, J.S., Lemieux, L.. - In: NEUROIMAGE. - ISSN 1053-8119. - 53:1(2010), pp. 196-205. [10.1016/j.neuroimage.2010.05.064]

Terms of use:

The terms and conditions for the reuse of this version of the manuscript are specified in the publishing policy. For all terms of use and more information see the publisher's website.

19/11/2026 02:08

(Article begins on next page)

3. Manuscript
Click here to view linked References

Title: Imaging haemodynamic changes related to seizures: comparison of EEG-based General Linear Model, Independent Component Analysis of fMRI and Intracranial EEG

R C Thornton[1*], R Rodionov[1*], H Laufs[1], S Vulliemoz[1], A Vaudano[1], D Carmichael[1], S Cannadathu[1], M Guye[2], A McEvoy[1], S Lhatoo[4], F Bartolomei[2], P Chauvel[2], B Diehl[1], F De Martino[5], RDC Elwes[3], M C Walker[1], J S Duncan[1] and L Lemieux[1]

[1] Dept of Clinical and Experimental Epilepsy, UCL Institute of Neurology, London WC1N 3BG, National Society for Epilepsy MRI Unit, Chalfont St Peter, Buckinghamshire SL9 0RJ

[2] CHU Timone, Service de Neurophysiologie Clinique, Marseille, F-13000, France and INSERM, U751, Marseille, F-13000, France

[3] Department of Clinical Neurophysiology, Kings College Hospital, London

[4] Department of Neurology, North Bristol NHS Trust, Frenchay, Bristol

[5] Department of Cognitive Neurosciences, Faculty of Psychology, University of Maastricht, Maastricht, The Netherlands

*These two authors contributed equally

Corresponding author: Louis Lemieux: l.lemieux@ion.ucl.ac.uk

Word Count: 4845

Abstract word count: 250

ABSTRACT

Background

Simultaneous EEG-fMRI can reveal haemodynamic changes associated with epileptic activity which may contribute to understanding seizure onset and propagation.

Methods

Nine of 83 patients with focal epilepsy undergoing pre-surgical evaluation had seizures during EEG-fMRI and analysed using 3 approaches, 2 based on the general linear model (GLM) and one using Independent Component Analysis (ICA):

1. EEGs were divided into up to 3 phases: early ictal EEG change, clinical seizure onset and late ictal EEG change and convolved with a canonical haemodynamic response function (HRF) (canonical GLM analysis).
2. Seizures lasting 3 scans or longer were additionally modelled using a Fourier basis set across the entire event (Fourier GLM analysis).
3. Independent Component Analysis (ICA) was applied to the fMRI data to identify ictal BOLD patterns without EEG.

The results were compared with intracranial EEG.

Results

The canonical GLM analysis revealed significant BOLD signal changes associated with seizures on EEG in 7/9 patients, concordant with the seizure onset zone in 4/7. The Fourier GLM analysis revealed changes in BOLD signal corresponding with the results of the canonical analysis in 2 patients. ICA revealed components spatially concordant with the seizure onset zone in all patients (8/9 confirmed by intracranial EEG).

Conclusion

Ictal EEG-fMRI visualises plausible seizure related haemodynamic changes. The GLM approach to analysing EEG-fMRI data reveals localised BOLD changes concordant with the ictal onset zone when scalp EEG reflects seizure onset. ICA provides additional information when scalp EEG does not accurately reflect seizures and may give insight into ictal haemodynamics.

INTRODUCTION

EEG-fMRI shows blood oxygen level dependent (BOLD) signal changes occurring with interictal epileptiform discharges (IEDs), which are concordant with the irritative zone in 60-70% of cases in whom IED are recorded (Al Asmi et al., 2003; Benar et al., 2006; Lazeyras et al., 2000; Salek-Haddadi et al., 2006; Seeck et al., 1998). fMRI studies of seizures are less common, but case reports and small series have shown ictal BOLD signal change both with (Donaire et al., 2009; Kobayashi et al., 2006; Salek-Haddadi et al., 2002; Tyvaert et al., 2008) and without (Detre et al., 1995; Federico et al., 2005) concurrent EEG.

In most EEG-fMRI studies of ictal activity, seizures have been represented as a single block across their duration convolved with an HRF (Kobayashi et al., 2006; Tyvaert et al., 2008) referring to the EEG for onset and offset times. In principle this single-block scalp EEG derived fMRI model is limited as:

1) Seizure onset is not always accurately detected by scalp EEG and may be delayed (Binnie and Stefan, 1999).

2) A single block may not accurately represent dynamic processes such as seizures (Niedermeyer et al 1999).

Furthermore, while the canonical HRF appears to be a suitable model in normal physiological conditions (Friston et al., 1995) and for IED-related BOLD signal changes (Lemieux et al., 2008), this has not been demonstrated for seizures. Flexible modelling methods have been used, such as those based on Fourier basis sets (Salek-Haddadi et al., 2006) or series of short blocks (Donaire et al., 2009; Tyvaert et al., 2009) addressing the potential complexity of ictal BOLD signal changes but they do not address the issue of how best to model these changes based on the available scalp EEG.

Given that ictal EEG does not always reflect seizure onset (Binnie and Stefan, 1999) providing localising information in 13-92% of patients (Blume, 2001; Foldvary et al., 2001; Lee et al., 2005), data driven analysis of fMRI (i.e. without modelling the EEG) may be helpful. Early ictal fMRI studies without EEG, found an increase in BOLD signal at or in advance of seizure onset

compared to baseline, within the presumed seizure onset zone (Detre et al., 1995)(Federico et al., 2005). Mathematically rigorous signal processing methods such as Independent Component Analysis (ICA) applied to simulated and interictal data, have demonstrated BOLD changes concordant with the results of traditional EEG-derived fMRI modelling techniques (Levan and Gotman, 2008; Rodionov et al., 2007) opening a new avenue for the investigation of seizure-related fMRI changes (Levan et al., 2010).

The main objective of the current study was to explore the BOLD signals related to epileptic seizures in a series of consecutive patients awaiting intracranial EEG as part of their pre-surgical evaluation. We chose to address the limitations of a single-block design GLM, by using two, more flexible modelling approaches:

1. Partition of the seizures into 3 EEG-defined blocks each convolved with a canonical HRF
2. Fourier basis set across the entire event for long seizures.

We used ICA combined with a component classifier [De Martino et al, 2007] to identify seizure related BOLD signal changes without reference to the EEG.

The findings of the three analyses were compared with intracranial EEG data.

MATERIALS AND METHODS

Patients

83 patients with refractory focal epilepsy undergoing pre-surgical evaluation including intracranial EEG (icEEG) at four centres (National Hospital for Neurology and Neurosurgery, London, UK, Kings College Hospital, London, UK, Frenchay Hospital, North Bristol NHS Trust, UK and Hopital de la Timone, Marseille, France) were studied. All procedures were subject to local Research and Development directorate guidelines and National Research Ethics Committee Approval in the UK and France.

Nine of the 83 patients had seizures during EEG-fMRI acquisition (determined by patient report, clinical observation and EEG). Eight of nine had subsequent intracranial EEG recording to localise the seizure onset zone; in the remaining patient the procedure was abandoned owing to intra-operative complications.

Patients underwent scalp video-EEG telemetry, clinical and psychological assessment along with 3T structural MRI according to the standard Epilepsy Protocol used at the National Hospital for Neurology and Neurosurgery. Clinical data are summarised in Table 1.

EEG-fMRI Acquisition

32 or 64 EEG channels were recorded using a commercial MR-compatible system (BrainAmp MR and Vision Analyzer, Brain Products GMbH, Gilching, Germany) and ECG was recorded with a single lead. Two 20-minute sessions of resting state EEG-fMRI were recorded. A third 20-minute session was recorded if tolerated. Each consisted of 404 T2*-weighted single-shot gradient-echo echo-planar images (EPI; TE/TR 30/3000 ms, flip angle 90: 43 2,5 mm interleaved slices, FOV: 24x24cm^2, matrix: 64x64) acquired continuously on a 3 Tesla Signa Excite HDX MRI scanner (General Electric, Milwaukee, WI, USA). Further details are given elsewhere (Vulliemoz et al., 2009) .

EEG pre-processing

MRI acquisition and pulse related artefact were removed offline from the EEG trace recorded during scanning (Allen et al., 1998; Allen et al., 2000) using a commercial EEG processing package (Brain Analyzer, Brain Products, Munich, Germany) and IED and seizures were coded by at least two independent observers. Seizures were divided into three phases, each defined by an onset time and duration as follows:

- Early ictal phase, defined as the earliest observable change on EEG. This phase was not identified in patients in whom clinical features evolved simultaneously or in advance of EEG change.
- Clinical ictal phase, defined as the onset of myogenic artefact and/or clinical manifestation of the seizure.
- Late ictal phase, defined by onset of high amplitude low frequency change following the seizure onset on EEG.

We identified 3 distinct phases in 5/9 patients (#1, 3, 4, 5, 9) and two phases in 2 patients (# 6, 7). A single phase was identifiable in patient 2. Inpatient 8 the seizure could not be modelled from the EEG as the clinical events had no EEG correlate (see Table 2).

fMRI pre-processing and GLM analysis

After discarding the first four image volumes (T1 saturation effects), the EPI time series were realigned, and spatially smoothed with a cubic Gaussian Kernel of 8 mm full width at half maximum. fMRI time-series data were then analysed using a GLM to determine the presence of regional IED-related BOLD changes.

Motion-related effects were included in the GLM as 24 regressors (6 scan realignment parameters and a Volterra expansion of these (Friston et al., 1996)). No dataset was discarded because of motion. An additional set of confound regressors was included to account for pulse-related signal changes (Liston et al., 2006)

To characterise head movements for each dataset, inter-scan motion data derived from the SPM scan-realignment process were summarised as the minimum, maximum, average inter-scan displacement and the number of events in which head movement exceeded 1 mm (Table 1).

Two EEG-based modelling approaches were used:

Canonical HRF

For each seizure type, up to three phases (described above) were included in the model as separate conditions to identify patterns of BOLD change associated with each phase. Each phase was represented by a block from onset to offset and convolved with the canonical haemodynamic response function and its temporal and dispersion derivatives, resulting in a total of three separate regressors for each phase. In addition, BOLD signal changes associated with IEDs were modelled (Salek-Haddadi et al., 2006). Two F contrasts were specified to assess significant BOLD changes:

1. Across all phases, allowing comparison with the results of Fourier basis set analysis;
2. Specific to each phase.

Effects were considered significant at a threshold of p=0.05 (Family-wise Error (FWE) correction for multiple comparisons).

The direction of the BOLD changes for any given cluster was determined by plotting the fitted response at the voxel with maximal t-score within the cluster and observing the event-related BOLD response.

Fourier Basis Set

In those cases (#1, 3, 4, 7 and 9) in whom seizures were long enough (longer than 3TR = 9 seconds), we attempted to model inter-regional variations in the temporal evolution of the BOLD signal during the seizure, using a model capable of capturing signal changes of arbitrary shape arising consistently across events. We used a Fourier basis set over a time window corresponding to the longest period common to all seizures within a patient. The number of Fourier basis functions was chosen according to the event duration so that the model's temporal resolution was constant across cases and events, determined by the term with the shortest wavelength which was set at 2TR (6 sec). Events that could not be modelled using Fourier regressors, for example those in which seizure length varied (see case 3), were included in the model using the canonical HRF approach

(above). A F contrast was used to assess ictal BOLD changes corresponding to any linear combination of the Fourier basis set functions, considered significant at $p<0.05$ (FWE) resulting in an SPM{F} map, which was compared with that obtained for the canonical HRF model.

For both the Canonical HRF and Fourier Basis Set approaches, the estimated time courses of event-related BOLD signal change were plotted for the most significant cluster and the cluster nearest to the seizure onset zone.

Comparison of the GLM results with intracranial data

In case 3, comparison was only possible with non-invasive data. In the other cases, patient-specific T1-weighted MRI scans were co-registered and fused with a post-operative CT with the sub-dural grid or depth electrodes in situ (Engel, 2001). These fused images were co-registered with the SPM{F} to identify regions of BOLD signal change in relation to the intracranial EEG. The degree of concordance of the GLM results was assessed based on the entire statistical maps: these were classified as follows:

- Concordant (C), when all significant BOLD clusters were concordant with the site of seizure onset identified on intracranial EEG, provided that the area of maximal signal change was in the same gyrus and within 2cm of the intracranial EEG electrode marking seizure onset , allowing for inaccuracies of co-registration and intra-operative brain shift (Nimsky et al., 2000)
- Concordant plus (C+) when the BOLD cluster containing the global statistical maximum was concordant but additional, discordant clusters were revealed
- Discordant (D), when no cluster was concordant or NULL, when no significant activation was revealed (Table 4).

Independent Component Analysis (ICA)

Spatial ICA (Formisano et al., 2004; McKeown et al., 2003) as implemented in Voyager QX software (Brain Innovation, Maastricht, Netherlands) was performed on fMRI data to reveal BOLD

patterns specific to the seizure onset zone and to study the time course of the BOLD signal change.

In summary, the technique constrains the analysis to grey matter and uses a fixed point ICA algorithm to separate signals generated by different sources (FastICA, Hyvärinen, 1999). Each fMRI dataset was decomposed on 80 spatially independent components (IC) following our previous demonstration that BOLD classified components were stable at this level of decomposition (Rodionov et al., 2007). ICs were overlaid on each patient's T1-weighted image in Talairach space.

Classification of independent components

Automatic IC classification sorted the components into:(De Martino et al., 2007): (1) 'BOLD' , including components which reflect normal physiological resting and task related brain states (Mantini et al., 2007; Raichle et al., 2001; Schmithorst and Brown, 2004); (2) EPI-susceptibility artefacts;(3) motion artefacts; (4) physiological noise; (5) noise at high spatial frequency; and (6) noise at temporal high frequency. We observed motion highly correlated with seizures in two patients (4 and 7), resulting in components with features of >1 of the above types, and undertook a further decomposition into 160 components to attempt to separate these components.

The classifier (Rodionov et al., 2007) (De Martino et al., 2007) was designed to be inclusive with respect to BOLD components to reduce the probability of misclassification of a BOLD-related IC. Components classified as BOLD or EPI low-frequency drift artefact, were inspected by an observer blinded to the clinical data, and divided into. 3 further subtypes according to their spatial pattern as follows:

1. Misclassified as BOLD (i.e. the spatial and temporal pattern suggested that the component should have been classified as noise)
2. Stereotypical of normal neuronal activity identified as known 'resting state networks' (Beckmann and Smith, 2004; Mantini et al., 2007), visual, auditory, motor, sensory.

3. ’Potentially epileptic’ (those exhibiting BOLD features, which do not fit 1 or 2)

Identification of ictal components

The fused images showing the intracranial electrodes were transformed to Talairach Space and the ‘potentially epileptic’ components identified using ICA were overlaid and reviewed to identify ‘ictal components’, based on their spatial relationship to the seizure onset zone defined on icEEG. When no ictal IC was identified among these, ICs in the other classes (motion, noise) were reviewed (potential ictal ‘non-BOLD’ ICs).

Correlation of GLM with IC time courses

We compared the EEG time course (as input to the GLM) with the signal time course of ‘ictal components’ by calculating the correlation coefficient between the EEG time course extracted from the fMRI model following convolution with the canonical HRF and the respective ictal IC time course. We calculated the correlation between both the ‘early ictal’ phase and the ‘total model’ across all phases (the most closely related to the seizure onset zone), and a representative ictal IC for each case.

RESULTS

Nine of 83 patients had seizures during EEG-fMRI. Four had frontal lobe epilepsy, two had temporal lobe epilepsy, one had parietal lobe epilepsy, one had occipital lobe epilepsy and one had a less well-defined posterior epilepsy. Between 1 and 5 seizures per patient were recorded during EEG-fMRI. Clinical data are summarized in table 1. The GLM and ICA analysis results are summarised below and in tables 2-5. Two representative cases are described (see figures 1,2). See supplementary web material for examples of the scalp EEG.

General Linear Model

See Table 2.

1. Canonical HRF

Significant BOLD signal changes were found in 7/9 cases using the canonical GLM. In 4 cases (cases #1, 2, 3, 5), BOLD localisation across all ictal phases was concordant with the seizure onset zone. In 5 cases (#1, 3, 4, 5, 7), there were significant BOLD changes linked to the early ictal EEG phase, which were concordant in 3 cases (#3-5). In 5/7 cases (#1, 3, 4, 5, 6), there were significant BOLD signal changes linked to the clinical phase of the seizure, concordant with seizure onset zone in two of these (#3 and 5). In 4/7 cases (#1, 3, 4, 5) significant BOLD changes were observed in relation to the late ictal phase, one of which (#5) was concordant with the seizure onset zone. In two cases (#1 and 3), BOLD localisation was discordant for one or all individual phases but concordant when all phases were considered together. In case #8, the ictal events could not be modelled in a GLM as the patient's seizures did not correlate with EEG change.

2. Fourier Basis Set

The Fourier basis set analysis showed significant BOLD signal changes in 3 of the 5 cases analysed (#1, 3 and 7); and the degree of concordance was the same as for the canonical HRF

analysis. In case 1, the global maximum was concordant with the seizure onset zone. In case #3, the most significant BOLD cluster was remote from the seizure onset but a smaller and less significant cluster was concordant with the structural lesion and presumed seizure onset. In case #7, the results were discordant. The temporal pattern of the BOLD signal revealed by the Fourier analysis varied between regions by shape and temporal delay of the high amplitude responses (see Figure 1).

Independent Component Analysis

Table 3 summarizes the ICA results.

The mean numbers of IC classified as BOLD and EPI per 20 min EEG-fMRI run were 7 (range 3-14) and 24 (range 14-36) respectively. Over both runs a mean of 6 ICs were characteristic of normal physiological activity (Beckmann and Smith, 2004; Laufs et al., 2003) and a mean of 4 BOLD IC per data set identified as 'potential epileptic components'.

Between 1 and 2 ICs spatially concordant with the seizure onset zone and classified as BOLD or EPI were observed in 5/9 cases. An IC spatially concordant with the seizure onset zone and classified as mixed BOLD/motion was observed in 1 case. In the remaining cases, at least one IC not classified as BOLD or EPI were observed spatially concordant with the seizure onset zone. In 8/9 cases, localisation was confirmed on intracranial data.

<u>Correlation of GLM and IC time courses</u>

See table 5 for a summary of the results. In 5 cases (#1, 2, 3, 5 and 7), the early ictal phase and/or total model (i.e. the {SPM-F} across all phases) was significantly ($p<0.001$) correlated with identified 'ictal' or 'potentially ictal non-BOLD' components'. The GLM model was most highly ($r>0.2$, $p<0.001$) correlated in cases #1, 3 and 5. In the remaining cases no phase of the EEG time course was significantly correlated with any ictal component. The 'late phase' and 'clinical phase' of the EEG were not significantly correlated with any ictal component in all but one (case #5) cases.

DISCUSSION

Using three different methods of ictal EEG-fMRI analysis we demonstrated:

- When the scalp EEG indicated the seizure onset, GLMs based on both the canonical HRF and Fourier basis set revealed patterns of ictal BOLD signal change concordant with the seizure onset zone on intracranial EEG.
- Although the yield of EEG-based GLM analysis was high, there were a number of cases in whom the EEG did not reflect the temporal evolution of seizures (# 4, 6, 8 and 9) and these did not demonstrate concordant BOLD signal change, illustrating the limitations of relying on a scalp-EEG derived model in ictal fMRI data.
- ICA identified spatially independent components, concordant with the seizure onset zone in all cases.
- When the scalp EEG accurately reflected seizure onset, the independent components were temporally correlated with the EEG model.
- Automatic classification identified BOLD or EPI components concordant with the seizure onset zone defined by intracranial EEG in 6/9 cases

Methodological Considerations

EEG-based GLM

The canonical GLM strategy assumes that BOLD signal changes follow a block-like time course at any voxel with a delay imposed by the canonical HRF (Friston et al., 1995). This has been used to reveal BOLD changes related to IED (Salek-Haddadi et al., 2006). Our three-phase model, based on the observation that in many cases ictal EEG starts from baseline, evolves in amplitude and frequency as the epileptic network is recruited and terminates with post-ictal slowing (Niedermeyer, 1999) allows for the evolution of haemodynamic changes between phases. Although this is not a perfect representation of the underlying neuronal activity (Binnie and Stefan, 1999), we suggest that this provides a more physiologically informed model than

either representing seizures as one continuous block or a series of short epochs of uniform length (Donaire et al., 2009; Tyvaert et al., 2009). The degree of concordance observed using this strategy was greatest for the early ictal phase and for the combined phases, than for either the clinical or late ictal phases, which is unsurprising given that seizure activity begins in one region and propagates to local and remotely connected cerebral areas.

The discrepancy between phase specific concordance and the concordance across all phases observed in two cases (#1 and 4) demonstrates that the SPM{F} for the combined map is based on the weighted sum of the individual effects, addressing the question "at which voxels do any linear combination (i.e. weighted sum) of the individual phases correlate with the signal?" in contrast to the phase specific SPM{F} which addresses the question "at which voxels does the block representing the phase correlate with the signal?". Given that our concordance criteria are based on the entire map and the global maximum, it is possible that a strong specific phase-related effect at one location does not match the combined effect of the 3 phases at another location.

The use of the Fourier basis set of regressors allows for wide inter-regional variation in time course reflecting the complexity of ictal haemodynamics. We restricted this approach to the longest ictal epoch >3TR common to each patient, to detect consistent, meaningful evolving patterns, given the temporal resolution of the technique.

In cases with multiple seizures our approach was designed to identify consistent patterns across events within each subject given consistent electrophysiological features across repeated seizures (Wendling et al., 1996), which increases statistical power.

Independent Component Analysis

ICA is limited by the large number of components generated, resulting in low specificity, which was addressed by the use of an automatic component classification scheme (De Martino et al., 2007) to reduce the number of candidate 'epileptic components'. In this study we considered the temporal characteristics of interictal and ictal events and therefore included components classified as EPI artefacts, to account for potential low-frequency ictal BOLD signal changes

(Federico et al., 2005; Tyvaert et al., 2008) and inspected all ICs spatially concordant with the seizure onset zone. This method differs from the approach of fitting an HRF to component time courses (Levan et al., 2010) .

In 4/9 patients (#3, 4, 6 and 9) 'ictal components' were not identified within the BOLD/EPI class, so we made a secondary decomposition into 160 components. In two patients (cases #4 and 7) in whom the EEG-fMRI recordings were contaminated by motion highly correlated with seizures, this resulted in the identification of further components classified as mixed BOLD and motion which were spatially concordant with the seizure onset zone. This demonstrates potential for ICA in analysing datasets contaminated by constant low amplitude motion, which causes difficulty in conventional fMRI data.

We expected to find 'BOLD' components with a spatial pattern involving sub-cortical structures, (Federico et al., 2005; Levan et al., 2010; Tyvaert et al., 2008), but none were observed. This may be because the classifier was trained for the cortex and sub-cortical components are generally smaller in size, so the degree of clustering on which ICA depends may not be comparable (Formisano, 2009).

Motion

The observed motion varied between 0-8mm (see Table 1). There was no apparent relationship between the amount of motion and degree of concordance of the GLM maps. The pattern of BOLD signal clusters observed on the combined phase SPM(F) was not typical of motion effects. In case #5 there was widespread BOLD signal change maximal at the seizure onset zone, which we hypothesise was due to focal seizure related effects added to spatially uniform motion related effects, consistent with previous reports of 'widespread intense BOLD signal change' in ictal fMRI (Kobayashi et al., 2006; Salek-Haddadi et al., 2002).

Neurophysiological Significance

<u>GLM</u>

All 4 cases (#1,2,3 &5) who had significant BOLD signal change concordant with the seizure onset zone had neocortical epilepsy and the earliest scalp EEG change was easily identified. In the 3 cases in whom icEEG was obtained the icEEG seizure onset was accurately reflected by the scalp EEG.

The lower degree of concordance than in previously published studies (Tyvaert et al., 2008), may reflect the fact that we analysed consecutive data sets in a cohort undergoing intracranial EEG, in whom scalp EEG was often not localising, restricting its value as a marker of neuronal activity on which to model fMRI data..

The lack of concordant ictal related BOLD signal in specific cases can be explained by region specific signal to noise ratio (case #9) or insensitivity of the scalp EEG to seizure onset (#4, 6 and 7). In case #3 a BOLD signal cluster posterior to the presumed site of seizure onset (left middle frontal gyrus and left superior temporal gyrus) was concordant with a left fronto-temporal IC which exhibited haemodynamic activity time-locked to ictal events on EEG. This cluster most likely represented propagation of the seizure, revealed by Fourier model. Similarly in case #7 the most significant cluster corresponded to a region of rapid seizure propagation on icEEG.

Clinical and late ictal phases

BOLD signal change concordant with seizure onset was observed mostly in relation to early ictal change or the whole seizure, although patterns suggestive of seizure propagation were observed in cases 3 and 6. We did not observe this in other cases as we compared each seizure phase with the baseline, rather than comparing BOLD signal change across phases (Donaire et al., 2009; Tyvaert et al., 2009).

BOLD decreases

Ictal-related BOLD decreases were observed, usually remote from the seizure onset zone or in regions reflecting the so-called Default Mode Network (DMN) (Raichle et al., 2001). BOLD decreases have previously been reported in the DMN related to IEDs in temporal lobe epilepsy

(Laufs et al., 2006) and generalised epilepsy (Archer et al., 2003; Hamandi et al., 2006) and are thought to reflect suspension of the resting state related to epileptic activity. Cases #1, 2 and 5 had mesial neo-cortical seizures with rapid EEG propagation, and BOLD decreases in the thalamus or basal ganglia. This is in keeping with involvement of these structures in seizures (Moeller et al.; Steriade et al., 1991; Vaudano et al., 2009). BOLD decreases were observed in relation to the late ictal phase in 3 cases, suggesting a cerebral perfusion/ metabolic demand mismatch resulting in sustained tissue hypoxia adjacent to the seizure focus despite, hyperoxygenation following the 'initial dip' within the focus (Zhao et al., 2009).

ICA

We identified ICs spatially concordant with the seizure onset zone in all cases. We hypothesise that the observed discrepancies between ictal IC and GLM derived maps result from the following:

1. Spatial smoothing was applied to data processed with the GLM, but not ICA
2. The two approaches are fundamentally different; GLM is restricted by the occurrence of EEG events whereas ICA results from the separation of signals.

Our findings of ICs spatially concordant with the seizure onset zone, complement a recent study in which spatially concordant ICs were identified in patients in whom a GLM analysis had previously revealed seizure-related changes (Levan et al., 2010) . We have extended the ICA approach by applying it to all cases regardless of the GLM approach and used the gold standard of icEEG for validation rather than the HRF. There was no consistent temporal relationship between seizures and component time courses, but in most cases where the time course of the EEG and IC were correlated the patients had neocortical epilepsy and the scalp EEG accurately reflected the seizure recorded on icEEG. In case #7, although the GLM result was discordant with the SOZ, there was rapid seizure propagation to the region of BOLD signal change, which may explain the temporal correlation observed between the ictal component and the 'discordant' GLM result. This is supported by the observation that the temporal resolution of fMRI means that

areas of IED and ictal onset and propagation may be seen in the same SPM (Vulliemoz et al., 2009) (Tyvaert et al., 2009).

In cases in whom the ictal ICs were not significantly correlated with the seizure model, the seizure onset recorded on icEEG was always in regions not well reflected on the scalp (insular cortex, basal temporal, mesial frontal and mesial temporal) resulting in the scalp EEG- based model being sub-optimal (Federico et al., 2005; Suh et al., 2006; Van Quyen et al., 2001; Zhao et al., 2007). In addition, neurovascular coupling may vary in ictal events (Zhao et al., 2009) (Salek-Haddadi et al., 2006). Inferences on the nature of the discrepancies between EEG onset and fMRI change beyond those accounted for by variation in HRF (Donaire et al., 2009; Tyvaert et al., 2009) are limited in the absence of an accurate measure of the event (e.g. simultaneous icEEG).

Clinical Relevance

EEG-fMRI can provide additional information about the haemodynamics of the ictal onset zone in patients undergoing pre-surgical evaluation even in the presence of large amount of head motion. The technique is unrestricted by the limited sampling and invasive nature of intracranial EEG (Engel, Jr. et al., 1990), allowing seizure-related haemodynamic changes to be observed throughout the brain. ICA was able to demonstrate spatially independent patterns concordant with seizure onset at a sub-lobar level in the majority of patients.

Although this suggests a possible role for ICA of fMRI in planning icEEG, the practicality of this approach is highly dependent on the number of components identified as potentially epileptic. The fact that the observed IC time courses only partially reflected the ictal changes on scalp EEG suggests that this non-invasive methodology can be a source of additional information, but also highlights uncertainty regarding the nature of the components, which requires further investigation. This may require refinement of the component classifier in particular addressing its specificity for ictal data. In addition to this, work should now focus on combining the EEG-informed and data-driven approaches to ictal fMRI to glean maximum information from this unique and rich data.

CONCLUSIONS

The analysis and interpretation of fMRI data acquired during seizures with concurrent EEG requires careful consideration in view of the limited ability of scalp EEG to model seizures and our limited knowledge of ictal haemodynamics. EEG-based models are successful in revealing significant BOLD changes in some cases, but the number of seizures captured and the location of the seizure onset zone have a significant impact on the results. When a GLM is not helpful, ICA can provide valuable information regarding the seizure onset zone, revealing complex patterns of signal change extending well beyond the events as seen on scalp EEG, raising new questions regarding the haemodynamics of seizures.

Acknowledgements

This work was funded by the Medical Research Council (G0301067).

This work was undertaken at UCLH/UCL who received a proportion of funding from the Department of Health's NIHR Biomedical Research Centres funding scheme and supported by a grant from the UK Medical Research Council no.G0301067. We are grateful to the Big Lottery Fund, Wolfson Trust and National Society for Epilepsy for supporting the NSE MRI scanner. HL was supported by the Deutsche Forschungsgemeinschaft (LA 1452/3-1) and the Bundesministerium für Bildung und Forschun. SV was supported by the "Fonds de Perfectionnement" of the University Hospital of Geneva, Switzerland. JD receives funding from the Wellcome Trust (067176) and the Medical Research Council (G9805089) and the National Society for Epilepsy. We thank Philippa Bartlett, Jane Burdett, Elaine Williams and Umair Chaudhary for help with scanning and all the patients who participated in the study. Thanks to Professor Elia Formisano PhD, of Maastricht University, for his support.

FIGURE LEGENDS

Figure 1:

Case 1: A 20 year-old female with left superior frontal gyrus focal cortical dysplasia. A single motor seizure of 48 seconds duration was recorded during EEG-fMRI. Ictal EEG consisted of rhythmic theta in both fronto-temporal leads (early ictal phase), myogenic artefact (clinical phase), and high amplitude delta (late ictal phase). Intracranial EEG (48 contact sub-dural grid over the left frontal and parietal lobes and 6-contact depth electrode recorded from the region of cortical dysplasia in the superior frontal gyrus) showed seizure onset within the dysplastic cortex extending to involve the motor hand area.

a) Results of canonical HRF GLM analysis overlaid on T1-weighted MRI fused with a CT containing sub-dural electrodes: the F contrast across all phases revealed maximal BOLD changes in the left superior frontal gyrus and pre-central gyrus ($p<0.05$ FWE corrected), with

further significant clusters at the inferior temporal borders. Individual phase related BOLD signal changes seen on the SPM {F} were remote from the seizure onset.

b) Results of Fourier basis set GLM analysis overlaid on T1-weighted MRI fused with a CT containing sub-dural electrodes: the seizure-related BOLD pattern was similar to that obtained for the canonical HRF across all phases but was more extensive.

c) Results of the canonical GLM seen in (a) overlaid on a surface rendering of the T1 weighted MRI illustrating the relationship of the BOLD signal change to the sub-dural electrodes. The sub-dural electrodes positions from fused T1-CT images in individual were co-registered with the T1 weighted image presented here for illustration.

d) Time course of the BOLD signal change over the course of the seizure (red, blue and green boxes delineate early, clinical and late ictal phases respectively).The time course for the cluster containing the global maximum reached maximal amplitude 11s after electrographic onset (5 s after clinical onset).

e) Results of ICA overlaid on T1-weighted MRI fused with a CT containing sub-dural electrodes: one BOLD IC was classified as ictal, with the largest cluster concordant with the seizure onset zone and additional, smaller clusters in the ipsilateral temporal lobe and contra-lateral frontal lobe. The time course of the IC was significantly correlated with the 'early ictal' model ($r=0.170$, $p=0.000$), the clinical ($r=0.21$, $p=0.000$) and the total model ($r=0.230$, $p=0.000$), but not correlated with the late ictal model ($r=0.08$, $p=0.13$).

f) Time course of the component illustrated in e) over the whole recording with the seizure indicated by the red box.

g) Independent component illustrated in (e) overlaid on a surface rendering of the T1-weighted MRI illustrating the relationship of the ictal onset zone and the component of interest. The sub-dural electrode positions from the fused T1-CT image were co-registered with the T1 weighted image presented here for illustration.

Figure 2:

Case 2: A 24 year-old male with right frontal cortical atrophy. Electrographic seizures were recorded during scanning consisting of prolonged continuous runs of right predominant bi-frontal spike/wave discharges. Intracranial EEG: 8 depth electrodes in the right hemisphere and 1 in the left, each with 15 contacts. Seven orthogonal electrodes (medial/lateral contacts): #1: orbito-frontal antero-medial/orbito-frontal lateral; #2: anterior cingulate gyrus/dorso-lateral prefrontal; #3: insula/fronto-opercular (pars opercularis); #4: insula/fronto-opercular (pars orbicularis); # 5: supplementary motor area/dorsal premotor cortex; #6: amygdala/middle temporal gyrus; #7: left hemisphere: anterior cingulate gyrus/dorso-lateral prefrontal. Two oblique electrodes: #8: right orbito-frontal postero-medial/ fronto-polar; #9: right dorsomedian thalamus /dorso-lateral-premotor. Seizure onset was observed in the mesial contacts of electrode 1 and 8 in mesial pre-frontal cortex concordant with the less significant BOLD cluster, rapidly involving the supplementary motor area (electrode 5).

a) Results of Canonical HRF GLM analysis overlaid on T1 weighted MRI fused with CT with intracranial electrodes: BOLD signal changes correlated with continuous spike-wave discharges were maximal in areas concordant with the seizure onset zone with additional right lateral frontal clusters. SPM{T}, $z = 6.98$ $p<0.05$, FWE (family wise error corrected for multiple comparisons)/

b) Results of Canonical HRF GLM analysis showing relationship of BOLD signal change to intracranial EEG. Contacts involved in seizure onset marked in green. Contacts in the irritative zone marked in red.

c) Results of ICA: Independent BOLD classified component overlaid on T1 weighted MRI fused with CT with intracranial electrodes, green ellipse indicates seizure onset zone from icEEG.

d) Time-course of the independent component shown in (c). Note lower frequency and higher amplitude of the BOLD signal, observed during the ictal epochs (marked by red boxes). The time course of the IC was significantly correlated with the EEG model ($r=0.141$, $p=0.002$).

Reference List

Al Asmi, A., Benar, C.G., Gross, D.W., Khani, Y.A., Andermann, F., Pike, B., Dubeau, F., Gotman, J., 2003. fMRI Activation in Continuous and Spike-triggered EEG-fMRI Studies of Epileptic Spikes. Epilepsia 44, 1328-1339.

Allen, P.J., Josephs, O., Turner, R., 2000. A Method for Removing Imaging Artifact from Continuous EEG Recorded during Functional MRI. NeuroImage 12, 230-239.

Allen, P.J., Polizzi, G., Krakow, K., Fish, D.R., Lemieux, L., 1998. Identification of EEG Events in the MR Scanner: The Problem of Pulse Artifact and a Method for Its Subtraction. NeuroImage 8, 229-239.

Archer, J.S., Abbott, D.F., Waites, A.B., Jackson, G.D., 2003. fMRI "deactivation" of the posterior cingulate during generalized spike and wave. NeuroImage 20, 1915-1922.

Beckmann, C.F., Smith, S.M., 2004. Probabilistic independent component analysis for functional magnetic resonance imaging. IEEE Trans.Med.Imaging 23, 137-152.

Benar, C.G., Grova, C., Kobayashi, E., Bagshaw, A.P., Aghakhani, Y., Dubeau, F., Gotman, J., 2006. EEG-fMRI of epileptic spikes: Concordance with EEG source localization and intracranial EEG. NeuroImage 30, 1161-1170.

Binnie, C.D., Stefan, H., 1999. Modern electroencephalography: its role in epilepsy management. Clin.Neurophysiol. 110, 1671-1697.

Blume, W.T., 2001. Current trends in electroencephalography. Curr.Opin.Neurol. 14, 193-197.

De Martino, F., Gentile, F., Esposito, F., Balsi, M., Di Salle, F., Goebel, R., Formisano, E., 2007. Classification of fMRI independent components using IC-fingerprints and support vector machine classifiers. NeuroImage 34, 177-194.

Detre, J.A., Sirven, J.I., Alsop, D.C., O'Connor, M.J., French, J.A., 1995. Localization of subclinical ictal activity by functional magnetic resonance imaging: correlation with invasive monitoring. Ann.Neurol. 38, 618-624.

Donaire, A., Bargallo, N., Falcon, C., Maestro, I., Carreno, M., Setoain, J., Rumia, J., Fernandez, S., Pintor, L., Boget, T., 2009. Identifying the structures involved in seizure generation using sequential analysis of ictal-fMRI data. Neuroimage. 47, 173-183.

Engel, J., Jr., Henry, T.R., Risinger, M.W., Mazziotta, J.C., Sutherling, W.W., Levesque, M.F., Phelps, M.E., 1990. Presurgical evaluation for partial epilepsy: Relative contributions of chronic depth-electrode recordings versus FDG-PET and scalp-sphenoidal ictal EEG. Neurology 40, 1670.

Engel, J., 2001. A Proposed Diagnostic Scheme for People with Epileptic Seizures and with Epilepsy: Report of the ILAE Task Force on Classification and Terminology. Epilepsia 42, 796-803.

Federico, P., Abbott, D.F., Briellmann, R.S., Harvey, A.S., Jackson, G.D., 2005. Functional MRI of the pre-ictal state. Brain 128, 1811-1817.

Foldvary, N., Klem, G., Hammel, J., Bingaman, W., Najm, I., Luders, H., 2001. The localizing value of ictal EEG in focal epilepsy. Neurology 57, 2022-2028.

Formisano, E., 2009. Personal Communication.

Formisano, E., Esposito, F., Di Salle, F., Goebel, R., 2004. Cortex-based independent component analysis of fMRI time series. Magnetic Resonance Imaging 22, 1493-1504.

Friston, K.J., Frith, C.D., Frackowiak, R.S.J., Turner, R., 1995. Characterizing Dynamic Brain Responses with fMRI: A Multivariate Approach. NeuroImage 2, 166-172.

Friston, K.J., Williams, S., Howard, R., Frackowiak, R.S., Turner, R., 1996. Movement-related effects in fMRI time-series. Magn Reson.Med. 35, 346-355.

Hamandi, K., Salek-Haddadi, A., Laufs, H., Liston, A., Friston, K., Fish, D.R., Duncan, J.S., Lemieux, L., 2006. EEG-fMRI of idiopathic and secondarily generalized epilepsies. NeuroImage 31, 1700-1710.

Kobayashi, E., Hawco, C.S., Grova, C., Dubeau, F., Gotman, J., 2006. Widespread and intense BOLD changes during brief focal electrographic seizures. Neurology 66, 1049-1055.

Laufs, H., Hamandi, K., Salek-Haddadi, A., Kleinschmidt, A.K., Duncan, J.S., Lemieux, L., 2006. Temporal lobe interictal epileptic discharges affect cerebral activity in "default mode" brain regions. Hum.Brain Mapp.

Laufs, H., Krakow, K., Sterzer, P., Eger, E., Beyerle, A., Salek-Haddadi, A., Kleinschmidt, A., 2003. Electroencephalographic signatures of attentional and cognitive default modes in spontaneous brain activity fluctuations at rest. Proc.Natl.Acad.Sci.U.S.A 100, 11053-11058.

Lazeyras, F., Blanke, O., Perrig, S., Zimine, I., Golay, X., Delavelle, J., Michel, C.M., de Tribolet, N., Villemure, J.G., Seeck, M., 2000. EEG-triggered functional MRI in patients with pharmacoresistant epilepsy. J Magn Reson.Imaging 12, 177-185.

Lee, S.K., Lee, S.Y., Kim, K.K., Hong, K.S., Lee, D.S., Chung, C.K., 2005. Surgical outcome and prognostic factors of cryptogenic neocortical epilepsy. Ann.Neurol. 58, 525-532.

Lemieux, L., Laufs, H., Carmichael, D., Paul, J.S., Walker, M.C., Duncan, J.S., 2008. Noncanonical spike-related BOLD responses in focal epilepsy. Hum.Brain Mapp. 29, 329-345.

Levan, P., Gotman, J., 2008. Independent component analysis as a model-free approach for the detection of BOLD changes related to epileptic spikes: A simulation study. Hum.Brain Mapp.

Levan, P., Tyvaert, L., Moeller, F., Gotman, J., 2010. Independent component analysis reveals dynamic ictal BOLD responses in EEG-fMRI data from focal epilepsy patients. Neuroimage. 49, 366-378.

Liston, A.D., Lund, T.E., Salek-Haddadi, A., Hamandi, K., Friston, K.J., Lemieux, L., 2006. Modelling cardiac signal as a confound in EEG-fMRI and its application in focal epilepsy studies. NeuroImage 30, 827-834.

Mantini, D., Perrucci, M.G., Del Gratta, C., Romani, G.L., Corbetta, M., 2007. Electrophysiological signatures of resting state networks in the human brain. Proceedings of the National Academy of Sciences 104, 13170-13175.

McKeown, M.J., Hansen, L.K., Sejnowsk, T.J., 2003. Independent component analysis of functional MRI: what is signal and what is noise? Current Opinion in Neurobiology 13, 620-629.

Moeller, F., Siebner, H.R., Wolff, S., Muhle, H., Boor, R., Granert, O., Jansen, O., Stephani, U., Siniatchkin, M., Changes in activity of striato-thalamo-cortical network precede generalized spike wave discharges. NeuroImage In Press, Corrected Proof.

Niedermeyer, E., 1999. Abnormal EEG Patterns: Epileptic and Paroxysmal. In: Niedermeyer, E., Lopes da Silva, F.H. (Eds.), Electroencephalography: Basic Principles, Clinical Applications and Related Fields, 4 ed. Lippincott Williams and Wilkins, Baltimore, pp. 235-260.

Nimsky, C., Ganslandt, O., Cerny, S., Hastreiter, P., Greiner, G., Fahlbusch, R., 2000. Quantification of, visualization of, and compensation for brain shift using intraoperative magnetic resonance imaging. Neurosurgery 47, 1070-1079.

Raichle, M.E., MacLeod, A.M., Snyder, A.Z., Powers, W.J., Gusnard, D.A., Shulman, G.L., 2001. Inaugural Article: A default mode of brain function. Proceedings of the National Academy of Sciences 98, 676-682.

Rodionov, R., De Martino, F., Laufs, H., Carmichael, D.W., Formisano, E., Walker, M., Duncan, J.S., Lemieux, L., 2007. Independent component analysis of interictal fMRI in focal epilepsy: Comparison with general linear model-based EEG-correlated fMRI. NeuroImage 38, 488-500.

Salek-Haddadi, A., Diehl, B., Hamandi, K., Merschhemke, M., Liston, A., Friston, K., Duncan, J.S., Fish, D.R., Lemieux, L., 2006. Hemodynamic correlates of epileptiform discharges: an EEG-fMRI study of 63 patients with focal epilepsy. Brain Res. 1088, 148-166.

Salek-Haddadi, A., Merschhemke, M., Lemieux, L., Fish, D.R., 2002. Simultaneous EEG-Correlated Ictal fMRI. NeuroImage 16, 32-40.

Schmithorst, V.J., Brown, R.D., 2004. Empirical validation of the triple-code model of numerical processing for complex math operations using functional MRI and group Independent Component Analysis of the mental addition and subtraction of fractions. NeuroImage 22, 1414-1420.

Seeck, M., Lazeyras, F., Michel, C.M., Blanke, O., Gericke, C.A., Ives, J., Delavelle, J., Golay, X., Haenggeli, C.A., de Tribolet, N., Landis, T., 1998. Non-invasive epileptic focus localization using EEG-triggered functional MRI and electromagnetic tomography. Electroencephalography and Clinical Neurophysiology 106, 508-512.

Steriade, M., Dossi, R.C., Nunez, A., 1991. Network modulation of a slow intrinsic oscillation of cat thalamocortical neurons implicated in sleep delta waves: cortically induced synchronization and brainstem cholinergic suppression. Journal of Neuroscience 11, 3200-3217.

Suh, M., Ma, H., Zhao, M., Sharif, S., Schwartz, T.H., 2006. Neurovascular coupling and oximetry during epileptic events. Mol.Neurobiol. 33, 181-197.

Tyvaert, L., Hawco, C., Kobayashi, E., Levan, P., Dubeau, F., Gotman, J., 2008. Different structures involved during ictal and interictal epileptic activity in malformations of cortical development: an EEG-fMRI study. Brain 131, 2042-2060.

Tyvaert, L., Levan, P., Dubeau, F., Gotman, J., 2009. Noninvasive dynamic imaging of seizures in epileptic patients. Hum.Brain Mapp.

Van Quyen, M., Martinerie, J., Navarro, V., Boon, P., D'Havθ, M., Adam, C., Renault, B., Varela, F., Baulac, M., 2001. Anticipation of epileptic seizures from standard EEG recordings. The Lancet 357, 183-188.

Vaudano, A.E., Laufs, H., Kiebel, S.J., Carmichael, D.W., Hamandi, K., Guye, M., Thornton, R., Rodionov, R., Friston, K.J., Duncan, J.S., Lemieux, L., 2009. Causal hierarchy within the thalamo-cortical network in spike and wave discharges. PLoS.One. 4, e6475.

Vulliemoz, S., Thornton, R., Rodionov, R., Carmichael, D.W., Guye, M., Lhatoo, S., McEvoy, A.W., Spinelli, L., Michel, C.M., Duncan, J.S., Lemieux, L., 2009. The spatio-temporal mapping of epileptic networks: combination of EEG-fMRI and EEG source imaging. Neuroimage. 46, 834-843.

Wendling, F., Bellanger, J.J., Badier, J.M., Coatrieux, J.L., 1996. Extraction of spatio-temporal signatures from depth EEG seizure signals based on objective matching in warped vectorial observations. IEEE Trans.Biomed.Eng 43, 990-1000.

Zhao, M., Suh, M., Ma, H., Perry, C., Geneslaw, A., Schwartz, T.H., 2007. Focal increases in perfusion and decreases in hemoglobin oxygenation precede seizure onset in spontaneous human epilepsy. Epilepsia 48, 2059-2067.

Zhao, M., Ma, H., Suh, M., Schwartz, T.H., 2009. Spatiotemporal Dynamics of Perfusion and Oximetry during Ictal Discharges in the Rat Neocortex. Journal of Neuroscience 29, 2814-2823.

4. Table

Table 1. Clinical Data.

	Epilepsy syndrome	**Semiology**	**IEDs in scanner**	**Ictal EEG in scanner**	**Structural MRI**	**Intracranial EEG**	**Head movements > 1 mm, # / min/ average/ max**
1	L FLE	R foot paraesthesia, R hand and foot jerks	Bilat runs of sharp theta, max amplitude in F3	1 event (50 sec long): high amplitude sharp waves, rhythmic theta	FCD, L Sup F gyrus	SOZ = IZ: L Sup F gyrus	-
2	R FLE	L head and eye deviation, vocalization	Bi-F spike wave discharge. (Max: F4-C4)	Continuous bi-F rhythmic spike-wave discharges max F4-C4	R F atrophy	SOZ = IZ: R pre-F cortex, ACC, R SMA	2/1.44/1.5/1.58
3	L FLE:	Loss of awareness, R upper limb jerking	L and R F sharp waves and spikes	5 events (21, 32, 21, 25, 59 sec long): Rapid discharges L F (max F3), rhythmic bilateral slowing	Left frontal gliosis (post traumatic)	N/A	15/1.0/2.9/6.1
4	R FLE:	L sided jerks, face and arm	R F theta (max C4)	4 events (111, 163, 147, 165 sec long): R F delta, rapid bilateral spread (max F4-P4).	R F-T lesion: unclear aetiology	R Inf F Gyrus and Sup T Gyrus	-
5	R PLE	L foot sensory disturbance, L head version, vocalization	R F slowing (max F4)	2 events (28, 19 sec long): 30 Hz activity at F4-C4, rhythmic slowing max at F4-C4	Normal	SOZ= IZ: R post-central gyrus	7/1.1/2.6/8.0
6	R T-Par epilepsy	Blinking, rapid loss of awareness, vocalization.	R P spikes and polyspikes (T8-P8)	3 events (15, 12, 66 sec long): R parietal fast, bilateral rhythmic discharge	FCD base R T, Par and Occ lobes	SOZ: R Inf T and P	-
7	R OLE	Visual hallucination (colours), blinking, oral automatisms	L T spikes (max F7). Bilateral post theta.	1 event (87 sec long): Blink aRifact followed by rhythmic bilateral delta	FCD R P and O lobes	SOZ: R O	-
8	R FLE	L foot and arm clonic jerks	R F spikes	Multiple clinical ictal events not related to EEG	Normal	SOZ: R medial F and P	3/1.7/3.9/5.6
9	L TLE	Ictal motor manifestation (inferred from myogenic aRefact on EEG)	None	1 event (33 sec long): Fast activity: L then R T.	L T atrophy	SOZ: L mesial T and T pole. Involvement of left lateral frontal lobe	5/1.0/1.5/2.7

Abbreviations:
R = right, L = left, IZ = irritative zone, SOZ = seizure onset zone, T – Temporal, F = Frontal, O = Occipital, P = Parietal Bi-F= Bifrontal, TLE = temporal lobe epilepsy, PLE = parietal lobe epilepsy, FLE = frontal lobe epilepsy. Inf = inferior Sup = superior. EEG= electroencephalogram FCD= Focal cortical dysplasia ACC= anterior cingulate cortex SMA= supplementary motor area
The ictal event durations are the sum of durations of early, clinical and late ictal phases.

Table 2: GLM analyses.

Case	Ictal phases used for modelling	Ictal canonical GLM				Ictal Fourier basis set
		Early ictal EEG	Clinical ictal EEG	Late ictal EEG	All phases combined	
1	Early / clinical / late	R F Orb, (+)	R F Orb, (+)	L mid-T, (-)	L sup F gyrus, (+)	L sup F gyrus, L and R inf T border, Th
2	Complete seizures	N/A	N/A	N/A	R F Orb, R mesial F (+), Th, DMN(-)	N/A
3	Early / clinical / late	L sup F gyrus, (+)	L middle F gyrus, (-)	L Occ, Biphasic (- then +)	L sup F gyrus; L post T, Th (-)	L inf F gyrus and L Par
4	Early / clinical / late	R Occ; bil mesial F (*), bi-phasic (neg-pos)	Bil mesial and lat F, (+)	R pre-central gyrus, (-)	R middle frontal gyrus, triphasic (pos-neg-pos)	NULL
5	Early / clinical/ late	Diffuse, Maximal R mesial P (+)	Diffuse, Maximal R mesial P (-)	Diffuse, Maximal R mesial P (+)	Diffuse, Maximal R mesial P (+)	N/A
6	Clinical/ late	N/A	R mesial pre-F cortex, (+)	NULL	R mesial pre-F cortex, (+)	N/A
7	Early /late	Bil Occ; L more significant, bi-phasic (neg-pos)	NULL	N/A	Bil Occ; L more significant, bi-phasic (neg-pos)	R T; L Occ
8	Not modelled	N/A	N/A	N/A	N/A	N/A
9	Early / clinical / late	NULL	NULL	NULL	NULL	NULL

All results were statistically significant after correction for multiple voxel comparisons ($p<0.05$); except (*): $p<0.001$, uncorrected.

Abbreviations:
R = right, L = left. FLE= frontal lobe epilepsy, TLE= Temporal lobe epilepsy, PLE = parietal lobe epilepsy, OLE = occipital lobe epilepsy. post = posterior DMN= default mode network Occ= occipital Orb= orbital sup= superior inf= inferior T= Temporal. N/A not applicable for the reasons that (a) no corresponding event observed on the EEG and (b) GLM using Fourier basis set was not used in these cases. NULL = no BOLD signal clusters on the SPM. The sign of the BOLD response is labelled as + (pos) and (-) (neg) for positive and negative BOLD signal changes in the canonical GLM analysis. N/A= not applicable.

Table 3: Results of ICA Analysis.

Case	Number of BOLD IC	Number of EPI IC	Number and classification of ictal IC	Saptially similar to SOZ on icEEG?
1	13	25	1: BOLD	Yes
2	9	36	2: BOLD	Yes
3	3	20	1: motion	N/A
4	3	15	1: BOLD + motion	Yes
5	14	14	2: BOLD	Yes
6	11	33	1: SDN	Yes
7	3	36	1: EPI	Yes
8	3	22	1: BOLD	Yes
9	3	17	1: tHFN	Yes

N/A= not applicable (no intracranial EEG); SDN=Spatially distributed noise; tHFN=temporal high-frequency noise; SOZ=seizure onset zone

Table 4. Concordance of GLM and ICA results with electro-clinical localisation

Case (# events)	Canonical GLM				**Fourier GLM**	**No of ICs spatially concoradant with SOZ**
	All phases	Early	Clinical	Late		
1 (1)	**C+**	D	D	D	**C+**	1
2(>20)	**C**	n/a	n/a	n/a	**n/a**	2
3 (5)	**C**	C	C	D	**C**	1(†)
4 (4)	**D**	C(*)	C	D	**NULL**	1
5 (2)	**C+**	C+	C+	C+	**n/a**	2
6 (3)	**D**	n/a	D	NULL	**n/a**	1(†)
7 (1)	**D***	D*	NULL	n/a	**D***	1
8(**)	**n/a**	n/a	n/a	n/a	**n/a**	1
9 (1)	**NULL**	NULL	NULL	NULL	**NULL**	1(†)

(*): only significant at p<0.001, uncorrected. (†): not amongst the BOLD or EPI components. (**) –clinical event had no scalp EEG correlate. C=concordant with seizure onset zone on intracranial EEG, C+= clusters concordant with seizure onset zone, but additional clusters were discordant. D= discordant with the seizure onset zone.

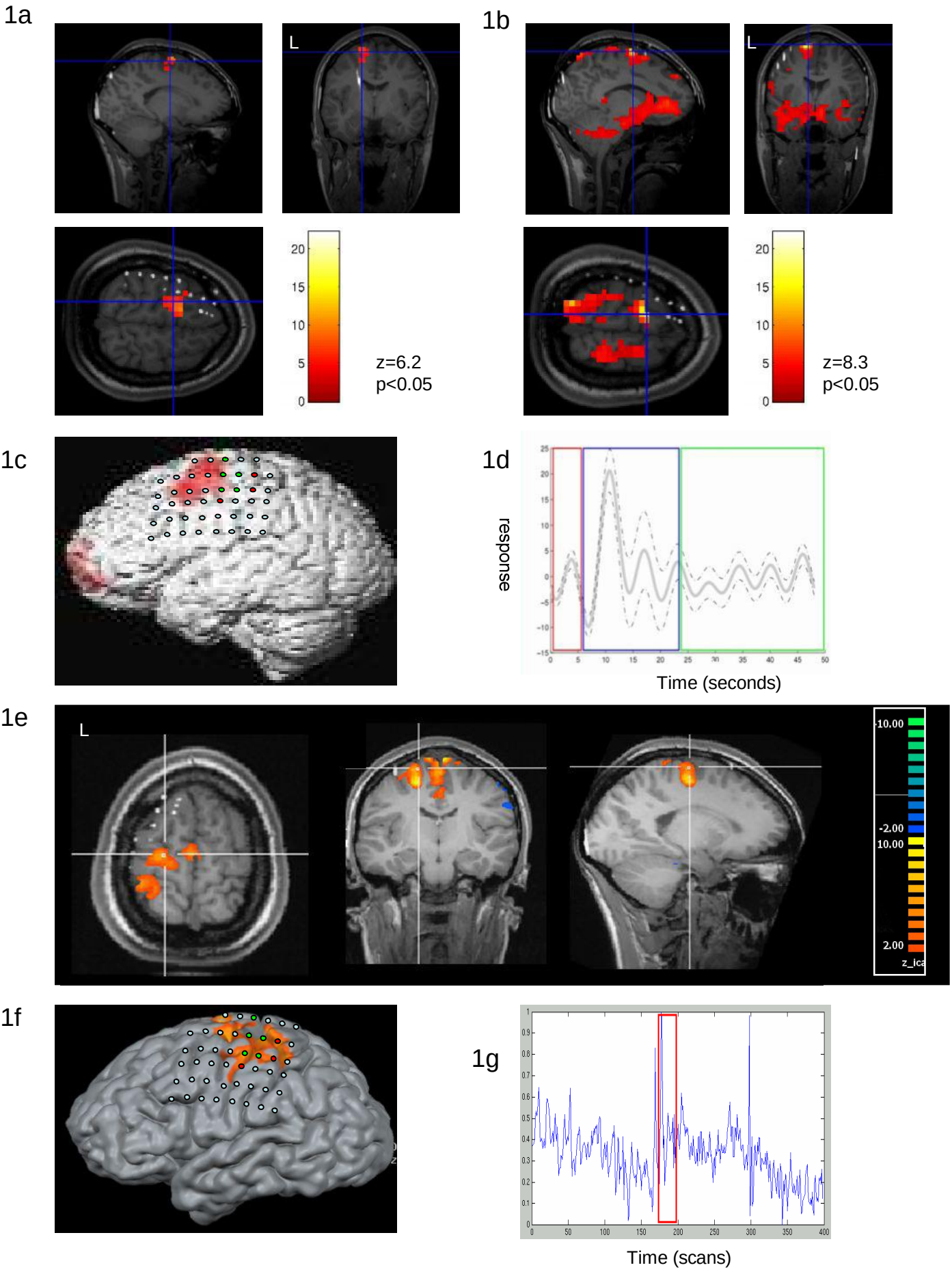
Table 5. Correlation between independent time course and EEG model used in GLM.

Case	**Early Ictal Phase**		**Total model (all phases combined)**	
	R	**P**	**R**	**P**
1	0.170	0.000	0.230	0.000
2	n/a	n/a	0.141	0.002
3	-0.474	0.000	-0.333	0.000
4	**-0.009**	**0.857**	**-0.077**	**0.126**
5	-0.123	0.014	-0.284	0.000
6	**-0.029**	**0.435**	**-0.083**	**0.324**
7	**0.148**	**0.005**	**0.144**	**0.004**
8	**n/a**	**n/a**	**n/a**	**n/a**
9	**-0.044**	**0.563**	**-0.325**	**0.000**

R= correlation coefficient. P= probability. Figures are rounded to nearest 0.001. n/a= not applicable, where the stated model did not apply to this dataset (see main text).

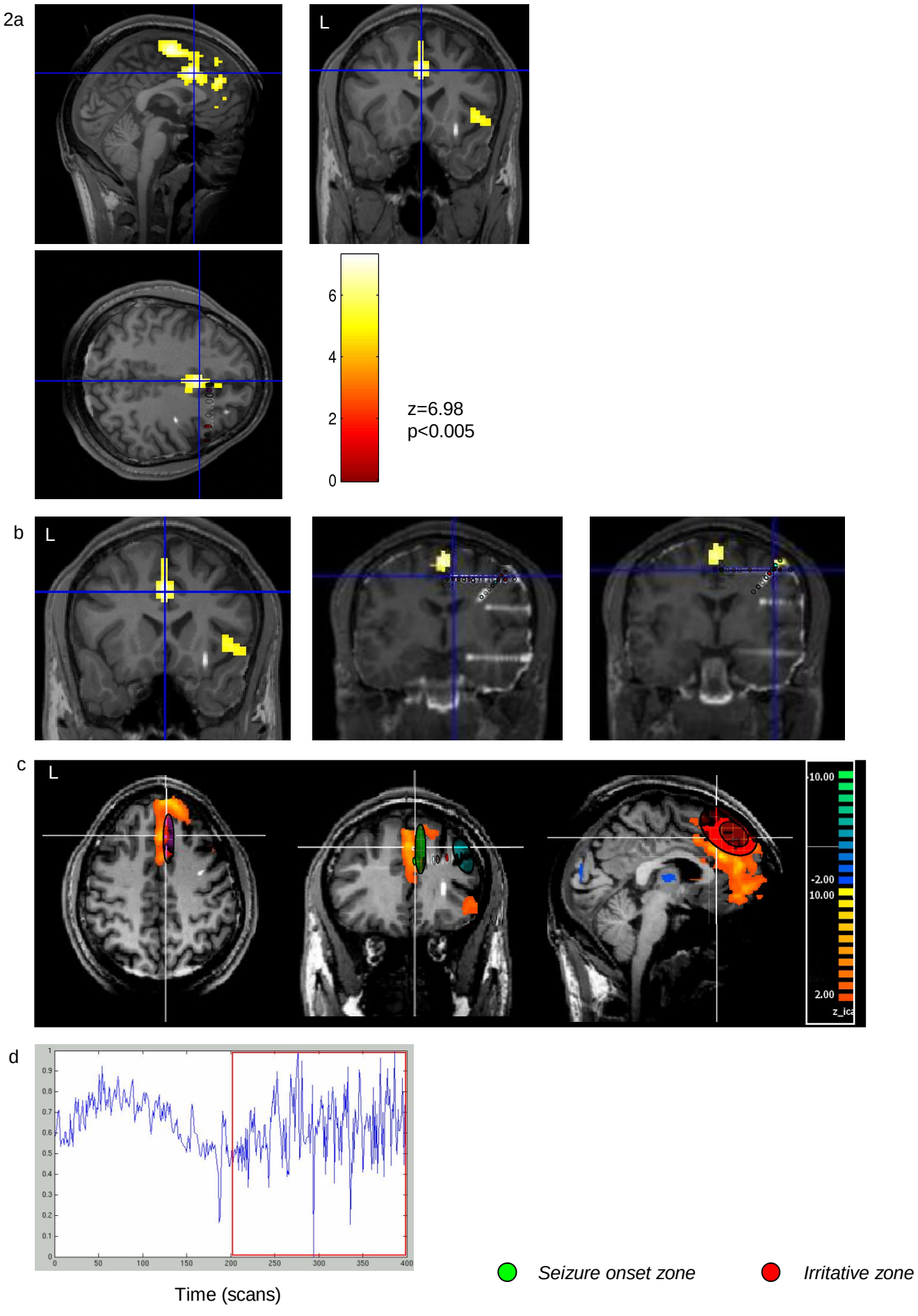
5. Figure

Click here to download 5. Figure: Figure1_revised.pdf



5. Figure

Click here to download 5. Figure: Figure2_revised.pdf



6. Supplementary Material

Click here to download 6. Supplementary Material: Figure1s_revised.pdf

6. Supplementary Material

Click here to download 6. Supplementary Material: Figure2s_revised.pdf

6. Supplementary Material

Click here to download 6. Supplementary Material: Figure3s_portrait.pdf

6. Supplementary Material

Click here to download 6. Supplementary Material: Figure4s_revised.pdf

6. Supplementary Material

Click here to download 6. Supplementary Material: Figure5s_revised.pdf

6. Supplementary Material

Click here to download 6. Supplementary Material: Figure6s_revised.pdf

6. Supplementary Material

Click here to download 6. Supplementary Material: Figure7s_revised.pdf

6. Supplementary Material

Click here to download 6. Supplementary Material: Supplementary_legends_NeuroImage_20100428.doc